

# blood

2013 121: 519-529  
Prepublished online December 3, 2012;  
doi:10.1182/blood-2012-05-432674

## Phosphatase Wip1 negatively regulates neutrophil development through p38 MAPK-STAT1

Guangwei Liu, Xuelian Hu, Bo Sun, Tao Yang, Jianfeng Shi, Lianfeng Zhang and Yong Zhao

---

Updated information and services can be found at:

<http://bloodjournal.hematologylibrary.org/content/121/3/519.full.html>

Articles on similar topics can be found in the following Blood collections

[Phagocytes](#), [Granulocytes](#), and [Myelopoiesis](#) (418 articles)

---

Information about reproducing this article in parts or in its entirety may be found online at:

[http://bloodjournal.hematologylibrary.org/site/misc/rights.xhtml#repub\\_requests](http://bloodjournal.hematologylibrary.org/site/misc/rights.xhtml#repub_requests)

Information about ordering reprints may be found online at:

<http://bloodjournal.hematologylibrary.org/site/misc/rights.xhtml#reprints>

Information about subscriptions and ASH membership may be found online at:

<http://bloodjournal.hematologylibrary.org/site/subscriptions/index.xhtml>

Blood (print ISSN 0006-4971, online ISSN 1528-0020), is published weekly by the American Society of Hematology, 2021 L St, NW, Suite 900, Washington DC 20036.

Copyright 2011 by The American Society of Hematology; all rights reserved.



## PHAGOCYTES, GRANULOCYTES, AND MYELOPOIESIS

## Phosphatase Wip1 negatively regulates neutrophil development through p38 MAPK-STAT1

\*Guangwei Liu,<sup>1,2</sup> \*Xuelian Hu,<sup>1</sup> \*Bo Sun,<sup>1</sup> Tao Yang,<sup>1</sup> Jianfeng Shi,<sup>1</sup> Lianfeng Zhang,<sup>3</sup> and Yong Zhao<sup>1</sup><sup>1</sup>State Key Laboratory of Biomembrane and Membrane Biotechnology, Institute of Zoology, Chinese Academy of Sciences, Beijing, China; <sup>2</sup>Department of Immunology, Shanghai Medical College, Fudan University, Shanghai, China; and <sup>3</sup>Key Laboratory of Human Diseases Comparative Medicine, Ministry of Health; Institute of Laboratory Animal Science, Chinese Academy of Medical Sciences and Peking Union Medical College, Beijing, China

## Key Points

- Phosphatase Wip1 negatively regulates neutrophil development.
- Wip1 regulates neutrophil development via p38 MAPK-STAT1.

Neutrophils are critically involved in host defense and tissue damage. Intrinsic molecular mechanisms controlling neutrophil differentiation and activities are poorly defined. Herein we found that p53-induced phosphatase 1 (Wip1) is preferentially expressed in neutrophils among immune cells. The Wip1 expression is gradually up-regulated during the differentiation of myeloid precursors into mature neutrophils. Wip1-deficient mice and chimera mice with Wip1<sup>-/-</sup> hematopoietic cells had an expanded pool of neutrophils with hypermature phenotypes in the periphery. The in vivo and in vitro studies showed that Wip1 deficiency mainly impaired the developing process of myeloid progenitors to neutrophils in an intrinsic manner. Mechanism studies showed that the enhanced

development and maturation of neutrophils caused by Wip1 deficiency were mediated by p38 MAPK-STAT1 but not p53-dependent pathways. Thus, our findings identify a previously unrecognized p53-independent function of Wip1 as a cell type-specific negative regulator of neutrophil generation and homeostasis through limiting the p38 MAPK-STAT1 pathway. (*Blood*. 2013;121(3):519-529)

## Introduction

Polymorphonuclear neutrophil granulocytes (PMNs or neutrophils) develop in the bone marrow (BM). They are fully equipped with a variety of granules, which contain proteases that enable the neutrophils to deliver lethal hits against invading microorganisms.<sup>1,2</sup> Although neutrophils are essential to host defense against intruding microorganisms and play a critical role in initiating inflammation and innate immunity, they also contribute to the pathology of various acute and chronic inflammatory conditions.<sup>3,4</sup> In this manner, means to properly control the development, homeostasis, and functional activities of neutrophils is of central importance to mounting robust host defense responses and simultaneously avoiding tissue damage.<sup>5,6</sup> However, the molecular mechanisms that accomplish this balanced effect remain poorly understood.

Wild-type (WT) p53-induced phosphatase 1 (Wip1, also called PP2C $\delta$ ), which is encoded by protein phosphatase magnesium-dependent 1 delta (PPm1D), is a serine/threonine protein phosphatase belonging to the type 2C $\delta$  protein phosphatases.<sup>7</sup> It is activated by various stresses and involved in various cellular processes, such as tumorigenesis and aging.<sup>8,9</sup> Wip1, overexpressed in many cancers, is recognized as a novel oncogene inhibiting several p53-dependent tumor suppressor pathways, such as ATM-CHK2-p53 and p38 MAPK-p53 pathways as well as the NF- $\kappa$ B pathway.<sup>10-13</sup> Currently, Wip1 is thought to be a promising drug target for cancer therapy. In the present study, after observing that Wip1 is specifically expressed in resting neutrophils among all

immune cells and is up-regulated gradually during neutrophil maturation, we used Wip1-deficient mice to investigate the role of Wip1 in neutrophil development and homeostasis. Notably, Wip1-deficient mice displayed neutrophilia with significantly expanded granulocytic differentiation and hypermaturation phenotype in a cell-intrinsic and specific manner. Thus, phosphatase Wip1, as a key feedback regulator, negatively controls granulocytopenia and peripheral neutrophil homeostasis.

## Methods

## Mice

C57BL/6 and CD45.1<sup>+</sup> mice were purchased from Beijing University Experimental Animal Center (Beijing, China). Wip1<sup>-/-</sup>, p53<sup>+/-</sup>, and p38<sup>+/-</sup> mice were kindly provided by the Key Laboratory of Human Diseases Comparative Medicine, the Ministry of Public Health (Beijing, China). Wip1<sup>-/-</sup> mice have been described<sup>10,14</sup> and backcrossed to the C57BL/6 background in our laboratory. Wip1<sup>-/-</sup> and p53<sup>+/-</sup> mice were mated to obtain Wip1<sup>-/-</sup>p53<sup>-/-</sup> double-knockout mice. All mice were bred and maintained in specific pathogen-free conditions. Sex-matched littermate mice 6-12 weeks of age were mainly used for experiments unless otherwise noted. Complete or mixed chimeras were generated by transferring 1 to 2  $\times$  10<sup>7</sup> BM cells (BMCs) from either WT and/or Wip1KO mice into lethally irradiated mice.<sup>15,16</sup> Animal protocols were approved by the Animal Ethics Committee of the Institute of Zoology, Beijing, China.

Submitted May 24, 2012; accepted November 11, 2012. Prepublished online as *Blood* First Edition paper, December 3, 2012; DOI 10.1182/blood-2012-05-432674.

\*G.L., X.H., and B.S. contributed equally to this study.

The online version of this article contains a data supplement.

The publication costs of this article were defrayed in part by page charge payment. Therefore, and solely to indicate this fact, this article is hereby marked "advertisement" in accordance with 18 USC section 1734.

© 2013 by The American Society of Hematology

## Flow cytometry

For flow cytometry analysis of surface markers, cells were stained with antibodies in PBS containing 0.1% (weight/volume) BSA and 0.1% NaN<sub>3</sub>. The antibodies were purchased from eBioscience: anti-CD34 (RAM34), anti-CD8a (53-6.7), anti-CD45R/B220 (RA3-6B2), anti-F4/80 (BM8), anti-CD116/32, (93) anti-Gr-1 (RB6-8C5), anti-CD45.1 (A20), and anti-CD45.2 (104). The following antibodies were purchased from BD Biosciences: anti-CD11b (M1/70) and anti-CD11c (HL3). The following were purchased from BioLegend: anti-CD48 (HM48-1) and anti-CD45 (30-F11). The following were purchased from Miltenyi Biotec: anti-CD3 $\epsilon$  (145-2C11), anti-CD19 (6D5), and anti-Ter119 (Ter-119).

Intracellular C/EBP $\alpha$  (14AA) and PU.1 (T-21) from eBioscience were analyzed by flow cytometry according to the manufacturer's instructions. For detection of phosphorylated signaling proteins, purified cells were activated with lipopolysaccharide (Sigma-L2280) or TNF- $\alpha$  (Sigma-T7539), were immediately fixed with Phosflow Perm buffer (BD Biosciences), were made permeable with Phosflow Lyse/Fix buffer (BD Biosciences) and were stained with antibody to p-Akt (Ser 473; D9E), p-Erk (Thr202 and Tyr204; 20A), p-STAT1 (Tyr701 and Ser727; 58D6), or p-S6 (Ser235 and Ser236; D57.2. 2E) from Cell Signaling Technology. Flow cytometry data were acquired on a FACSCalibur (BD Biosciences) or Beckman Coulter Epics XL, and these data were analyzed with CellQuest Version 5.1 software. Cell numbers of various populations were calculated by multiplication of the total cell number by the percentages of each individual population from the same mouse, followed by averaging.

## Isolation of mature and progenitor populations from BMCs

BM was obtained as described before.<sup>16</sup> Granulocyte-monocyte progenitors (GMPs) were sorted according to published procedures.<sup>17,18</sup> For GMP isolation, BMCs were stained with lineage markers (anti-CD3 $\epsilon$ , anti-CD4, anti-CD8 $\alpha$ , anti-CD45R, anti-Gr-1, anti-CD19, anti-CD11b, and anti-TER119) as well as anti-c-kit, anti-sca1, anti-Fc $\gamma$ RII/III and anti-CD34 mAbs. Lin<sup>-</sup>sca1<sup>-</sup>c-kit<sup>+</sup>CD34<sup>hi</sup>Fc $\gamma$ RII/III<sup>hi</sup> cells were sorted. For neutrophil isolation, Ly6G<sup>+</sup>CD11b<sup>+</sup>F4/80<sup>-</sup> cells were sorted by FACSARIA II (BD Biosciences). For monocyte/macrophage isolation, Ly6G<sup>-</sup>CD11b<sup>+</sup>F4/80<sup>+</sup> cells were sorted. Purity and viability of cell populations exceeded 95%.

## BrdU incorporation assays

For the in vivo BrdU incorporation experiments, 150  $\mu$ L of a 10-mg/mL BrdU solution was injected intraperitoneally into mice. Mice were then bled and BMCs were isolated at the indicated time points, erythrocytes lysed, and BrdU<sup>+</sup> cells were visualized with the BrdU flow kit from BD Biosciences PharMingen using an FITC-labeled anti-BrdU antibody. Samples were also stained with Ly6G-PE to visualize neutrophils. Flow cytometry data were acquired on a FACSCalibur (BD Biosciences) or Beckman Coulter Epics XL, and the data were analyzed with CellQuest Version 5.1 software or FlowJo Version 7.6.5 software (TreeStar).

## Methylcellulose colony-forming assays

A total of 50 000 BMCs were cultured in methylcellulose (Methylcellulose Base Medium, R&D Systems) supplemented with recombinant murine G-CSF at indicated concentrations. Cells were cultured in triplicate for each concentration at 37°C and 5% CO<sub>2</sub> for 6 days, after which colony numbers were counted. For experiments with sorted GMP, 500 cells were placed in MethoCult M3231 supplemented with 50 ng/mL SCF, 10 ng/mL IL-3, and 25 ng/mL GM-CSF or 20 ng/mL G-CSF (StemCell Technologies). Colonies were counted and analyzed phenotypically after 8 days of cultures as described.<sup>19</sup>

## RNA and protein analyses

Real-time PCR was performed with probe sets from Applied Biosystems, and the target gene mRNA expression was normalized against the endogenous control gene HPRT as reported.<sup>15</sup> The used primers were summarized in Table 1. Fold change was calculated as  $2^{-\Delta\Delta C_t}$  (cycle threshold) for the difference between the C<sub>t</sub> value for the gene of interest and the respective C<sub>t</sub> value for HPRT1. Immunoblot was performed with the following antibodies: Wip1 (H-300), p-S6 (Ser235/236), p-Akt (Ser473), p-AKT (Thr308), p-STAT1 (Ser727), p-Erk (Thr202/Tyr204), C/EBP $\alpha$

**Table 1. Sequences of the used primers**

Genes	Forward primer	Reverse primer
<i>Cebp-<math>\alpha</math></i>	aur aca vac oga rcg agg aga	gcg gtc att gtc act ggt c
<i>Cebp-<math>\beta</math></i>	tga tgc aat ccg gat caa	cac gtg tgt tgc gtc agt c
<i>CSF3R</i>	cat ttt cca ggg cat act tt	cca gtag ggt cgg ttt ctt gt
<i>P53</i>	cat gaa ccg ccg acc tat c	tcc cgg aac atc tcg aag c
<i>PU.1</i>	atc gga tga ctt ggt tac tta c	ggt tct cag gga agt tct caa
<i>Gata1</i>	gaa tcc tct gca tca aca agc	ggg caa ggg ttc tga ggt
<i>Wip1</i>	ctg act gat agc cct act tac aac a	gag aag gca tta ctg cga aca
<i>Hprt1</i>	cct aag atg agc gca agt tga a	cca cag gac tag aac acc tgc taa

(14AA), C/EBP $\beta$  (47A1), C/EBP $\epsilon$  (C22), and  $\beta$ -actin (Sigma-Aldrich) were purchased from Cell Signaling Technology or Santa Cruz Biotechnology.<sup>20</sup>

## In vitro bactericidal activity by neutrophils

BM neutrophils were sorted as described in the previous paragraph. *Escherichia coli* strain (RFP-BL21) was grown overnight at 37°C, washed in PBS, and counted. Suspension of *E coli* containing a bacterial concentration corresponding to 10<sup>6</sup> colony-forming units (CFU) was incubated with or without 5  $\times$  10<sup>5</sup> neutrophils in flat bottom 96-well plates (Costar Life Sciences) in a total of 200  $\mu$ L of RPMI media at 37°C in 5% CO<sub>2</sub> for 3 hours. For phagocytosis experiments, neutrophils were collected and cultured with antimouse Fc $\gamma$ R mAb (clone 2.4G2) to block nonspecific staining and then stained with anti-Ly6G-FITC (eBioscience) at 4°C. After washing with cold PBS 3 times, the phagocytosis percentages of gated Ly6G<sup>+</sup> cells were determined using a FACS scan. For *E coli* survival experiments, sample wells were treated with 0.01% Triton X-100 for 5 minutes to lyse neutrophils and then washed twice with 100  $\mu$ L PBS. Surviving *E coli* CFUs were determined, and the survival was calculated as *E coli* number incubated with neutrophils divided by *E coli* number incubated without neutrophils.

## Oxidative burst assay

Respiratory burst was determined as described.<sup>21</sup> Neutrophils isolated from BM were incubated in the presence of 1  $\mu$ M dihydrorhodamine (Molecular Probes, Sigma-D1054) during stimulation with PMA (Sigma-P8139). Samples were incubated at 37°C for 15 minutes before immediate flow cytometric analysis. Neutrophils were defined by staining anti-CD11b and anti-Ly6G mAbs.

## Histologic analyses

Peripheral blood smears were stained with Giemsa protocol. Peripheral blood smears were photographed on a 2-photon laser scanning microscope (LSM510, Carl Zeiss) with a 100 $\times$ /0.30 numeric apheric aperture oil immersion lens and an RT Slider SPOT 2.3.1 camera (Diagnostic Instruments) using SPOT Advanced software (Version 3.5.9).

## Electron microscopy

High-pressure freezing and freeze substitution of neutrophils were performed as described previously.<sup>22</sup> The ultrathin sections were analyzed in a Philips 400 TEM at 80 kV.

## STAT1 knockdown with RNAi

A gene-knockdown lentiviral construct was generated by subcloning gene-specific short hairpin RNA sequences into lentiviral shRNA expression plasmids (pLL3.7). The following gene-specific targeting sequences were used to knockdown STAT1: GCC GAG AAC ATA CCA GAG AAT. Lentiviruses were harvested from culture supernatant of 293T cells transfected with 4  $\mu$ g shRNA vector, 3  $\mu$ g psPAX2, and 3  $\mu$ g pMD2.G. BMCs were infected with recombinant lentivirus, and green fluorescent protein expressing cells were isolated using fluorescence sorting 48 hours later. The STAT1 expression was confirmed using Western blots. The sorted GMPs with either control or shRNA vectors were used for methylcellulose colony-forming assays as described in the previous paragraph.

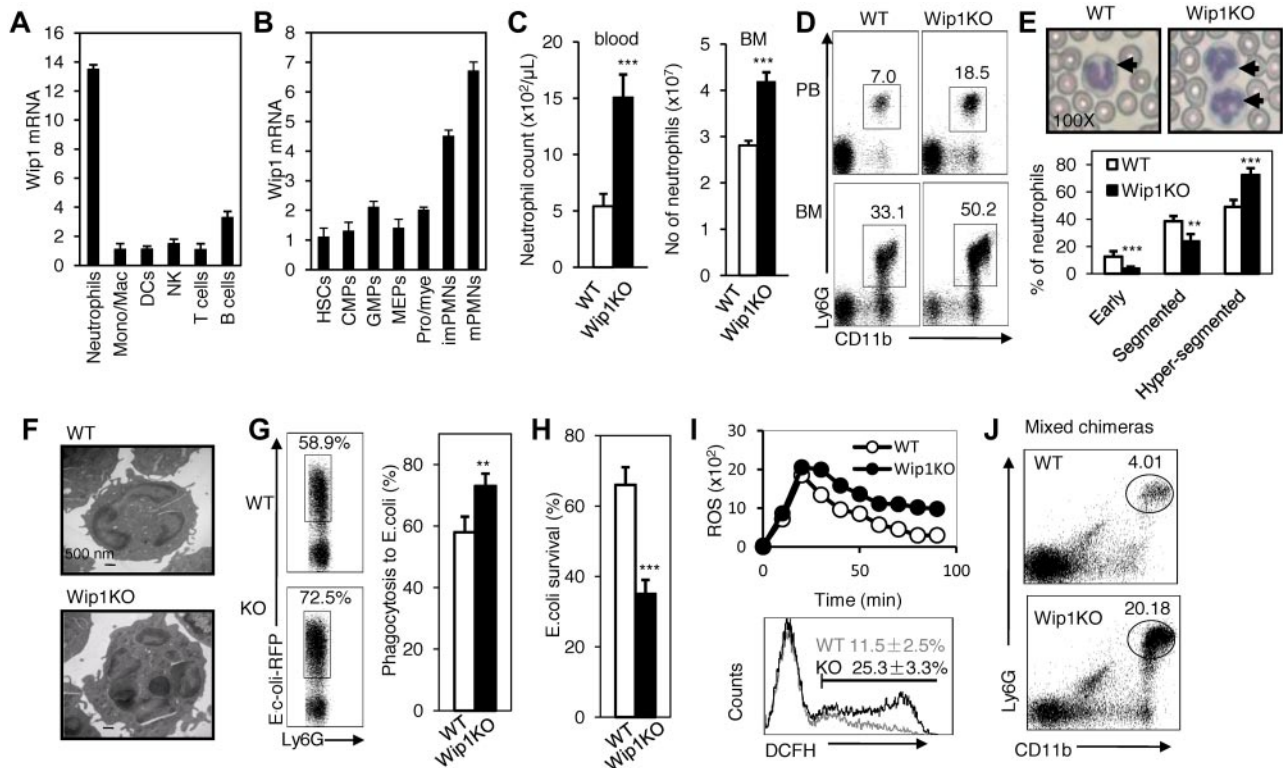


**Figure 1. The expression of Wip1 in immune cells and phenotypic characterization of myeloid cell population of Wip1-deficient mice were determined.** (A) Quantitative PCR analysis of Wip1 expression in the different subtypes of immune cell types (mean  $\pm$  SD,  $n = 3$ ). (B) Quantitative PCR analysis of Wip1 expression during neutrophil development from HSCs (mean  $\pm$  SD,  $n = 3$ ). (C) Bar graphs represent the total numbers of neutrophils in peripheral blood and BM of WT or Wip1KO mice. Values represent mean  $\pm$  SD,  $n = 15$  mice of each genotype.  $***P < .001$ , WT versus Wip1KO. (D) Representative FACS analysis of peripheral blood and BM CD11b<sup>+</sup>Ly6G<sup>+</sup> neutrophils. (E) Top: Morphologic analysis of peripheral blood neutrophils with Giemsa staining (original magnification  $\times 100$ ). Bottom: Quantitative assessment of nuclear segmentation scored in at least 50 neutrophils per animal. Blood smears from 5 mice of each genotype were morphologically analyzed and the extent of nuclear segmentation scored in at least 50 neutrophils per animals.  $**P < .01$ , WT versus Wip1KO.  $***P < .001$ , WT versus Wip1KO. (F) Morphologic analysis of WT and Wip1-deficient neutrophils with transmission electron micrograph was shown (original magnification  $\times 890$ ). (G) The neutrophil defense response to bacterial infection was determined in vitro. Neutrophils isolated from WT or Wip1KO mice were cultured with *E. coli*. The percentage of phagocytosis neutrophils was determined by FACS. The survival of bacteria in the culture was determined as described in "Methods." (H) The *E. coli* survival ratios were assayed after coculture of *E. coli* with WT or Wip1KO neutrophils. The experiments were performed in triplicate. (I) Respiratory burst by isolated BM neutrophils as measured by oxidation of dihydrorhodamine 123 after activation with 40 ng/mL PMA. Data represent the mean fluorescent intensity of all cells (mean  $\pm$  SD,  $n = 3$ , top). Bottom panel: Representative histogram showing the percentage of dihydrorhodamine-positive cells after incubation of neutrophils with 40 ng/mL PMA for 30 minutes. (J) Wip1KO CD11b<sup>+</sup>Ly6G<sup>+</sup> neutrophils were increased in mixed chimeric mice, which were generated by transplanting CD45.2<sup>+</sup> Wip1KO BMCs mixed with CD45.1<sup>+</sup> WT BMCs at the ratio of 1:1 into lethally irradiated CD45.1<sup>+</sup> mice. Representative results are shown from one of 3 independent experiments performed.

## Statistical analysis

All data are presented as the mean  $\pm$  SD. Student unpaired *t* test for comparison of means was used to compare groups.  $P < .05$  was considered to be statistically significant.

## Results

### Characterization of Wip1 expression in neutrophils

We initially detected the expression of Wip1 in different immune cell subsets. Neutrophils expressed the highest level of Wip1 compared with other immune cell subsets, including T cells, B cells, and monocytes/macrophages as detected by real-time PCR (Figure 1A), whereas the housekeeping gene HPRT mRNA levels were identical among these cells (supplemental Figure 1A, available on the Blood Web site; see the Supplemental Materials link at the top of the online article). The high level of Wip1 expression in neutrophils was further confirmed by Western blot assay (supplemental Figure 1B). To dissect the potential intrinsic role of Wip1 in hematopoietic differentiation, we evaluated its expression throughout myeloid development in highly purified cell populations from

BM. As granulocytic differentiation proceeds in BM through GMPs (CD34<sup>hi</sup>CD16/32<sup>hi</sup>), CD11b<sup>int</sup>Gr-1<sup>int</sup> promyelocytes/myelocytes, CD11b<sup>low</sup>Gr-1<sup>hi</sup> immature neutrophils (imNeu), and CD11b<sup>hi</sup>Gr-1<sup>hi</sup> mature neutrophils (mNeu),<sup>23,24</sup> the expression of Wip1 steadily increases, whereas hematopoietic stem cells (HSCs) and progenitor cells expressed relatively low levels of Wip1 (Figure 1B). Similar mRNA levels of housekeeping gene HPRT in these cells were observed (supplemental Figure 1C). The highest level of Wip1 protein expression in mNeu was determined by Western blot assays compared with promyelocytes/myelocytes and immature neutrophils (supplemental Figure 1D). The observation showing that the expression of Wip1 progressively increased with neutrophil differentiation from progenitor cells in a highly lineage-specific pattern promoted us to propose that Wip1 might be an important intrinsic modulator for neutrophil development, and homeostasis.

### Wip1-deficient mice displayed severe neutrophilia

To test this hypothesis, we used Wip1-deficient mice in the present study. In Wip1 knockout (Wip1KO) mice, wip1 expression is eliminated via gene targeting (supplemental Figure 2A), as

reported previously.<sup>10</sup> Immune blot and RT-PCR analysis demonstrated efficient deletion of Wip1 in BM neutrophils (supplemental Figure 2B-C). To access the requirement of Wip1 in the development of neutrophils, we analyzed the absolute cell number and cell percentage of neutrophils in the BM (per 2 femurs and 2 tibias) and peripheral blood of 6- to 8-week-old male WT and Wip1-deficient mice. Wip1KO mice had identical total cell numbers of white blood cells and BMCs as age-matched WT mice (supplemental Figure 3). Unexpectedly, the absolute cell number of circulating neutrophils increased ~3-fold in 4- to 6-week-old Wip1-deficient mice:  $15.1 \times 10^5$  cells/mL in Wip1-deficient mice versus  $5.4 \times 10^5$  cells/mL in controls ( $P < .001$ ; Figure 1C). Consistently, a markedly increased cell number of BM neutrophils were detected in Wip1-deficient mice ( $4.2 \times 10^5$  cells in Wip1-deficient mice vs  $2.8 \times 10^5$  cells in WT controls,  $P < .001$ ; Figure 1C). Flow cytometric analysis of peripheral blood and BMCs also confirmed the neutrophilia in Wip1-deficient mice (Figure 1D). Morphologic analyses assayed by May-Grunwald-Giemsa stain and transmission electron microscopy also revealed an unusual hypersegmentation morphology of neutrophils in Wip1-deficient mice characterized by nuclear hypersegmentation and blebbing ( $P < .01$ , Figure 1E-F). Consistent with the hypersegmentation phenotypes, Wip1-deficient neutrophils showed enhanced phagocytosis of bacteria ( $P < .01$ , Figure 1G-H) and produced more reactive oxygen species (Figure 1I) compared with WT controls. These data collectively indicate that Wip1 deficiency intrinsically promotes the hypermature phenotype of neutrophils.

Does Wip1 affect the neutrophil population intrinsically? When we adoptively transferred WT or Wip1-deficient BMCs into lethally irradiated syngeneic recipients to establish full hematopoietic chimeras, significantly higher percentages and cell number of neutrophils were observed in recipients who received Wip1-deficient BMCs than in those who received WT BMCs (supplemental Figure 4A-B). Conversely, Wip1-deficient mice grafted with WT BMCs showed similar level of neutrophils in peripheral blood and BM as WT mice got WT BMCs (supplemental Figure 4C-D). In addition, we generated mixed hematopoietic chimeras by performing competitive repopulation assays in which lethally irradiated syngeneic WT CD45.1<sup>+</sup> mice were cotransplanted  $1 \times 10^6$  CD45.1<sup>+</sup> WT BMCs with either  $1 \times 10^6$  CD45.2<sup>+</sup> Wip1-deficient or CD45.2<sup>+</sup> WT BMCs. Most of the circulating neutrophils in mice receiving WT plus Wip1-deficient BMCs were of Wip1-deficient donor origin ( $82\% \pm 13\%$  CD45.2<sup>+</sup> Wip1KO vs  $18\% \pm 9\%$  CD45.1<sup>+</sup> WT neutrophils), whereas recipients of CD45.1<sup>+</sup> plus CD45.2<sup>+</sup> WT BMCs displayed ~1:1 ratio of peripheral neutrophils (Figure 1J; supplemental Figure 4E-H). Because the presence of WT BMCs and immune cells in the same host failed to “rescue” the neutrophilia caused by Wip1 deficiency, we concluded that Wip1 is important for regulating neutrophil maturation and peripheral granulocyte compartment pool in a cell-autonomous manner.

#### Loss of Wip1 expression promotes differentiation of myeloid progenitor cells

The neutrophilia of Wip1-deficient mice might be the result of a decrease of cell death and/or an increase in the differentiation of neutrophils from progenitors. To address the first possibility, we detected the cell death rate of neutrophils by combining annexin V and propidium iodide staining. Wip1-deficient mice revealed normal cell death kinetics of freshly isolated neutrophils as WT mice after different periods of culture (Figure 2A-B). In addition, the cell death ability of promyelocytes/myelocytes and immature

and mature neutrophils was comparable between cells isolated from WT and Wip1KO mice (supplemental Figure 5A). Thus, it is unlikely that Wip1 regulates the survival of mature neutrophils. We next performed 5-bromodeoxyuridine (BrdU) incorporation studies to exhibit the neutrophil generation and homeostasis. The percentage and absolute cell number of BrdU<sup>+</sup> neutrophils were significantly higher in peripheral blood and BM of Wip1-deficient mice compared with the controls ( $P < .001$ , Figure 2C-F). In the competitive repopulation assays of mixed chimeras, Wip1-deficient BMCs developed into 2-3 times more BrdU<sup>+</sup> immature and mature neutrophils compared with the cotransferred CD45.1<sup>+</sup> WT cells in the same hosts 96 hours after BrdU injection ( $P < .001$ , Figure 2G-H). In addition, we detected the BrdU<sup>+</sup> cells in promyelocytes/myelocytes as well as immature and mature neutrophils in vivo. The major proliferating cells were among the promyelocyte/myelocyte population (supplemental Figure 5B). However, BM mature neutrophils showed certain levels of BrdU<sup>+</sup> cells (~20%), which could be derived from either myelocytes that incorporated BrdU during their last division or from myeloid progenitors/precursors that may have divided since incorporating BrdU<sup>25</sup> (supplemental Figure 5B). Nevertheless, Wip1-deficient promyelocyte/myelocyte cells displayed a higher proliferation ability compared with WT controls ( $P < .001$ , supplemental Figure 5B). Enhanced percentages of BrdU<sup>+</sup> cells in immature and mature neutrophils were also observed in Wip1KO mice (supplemental Figure 5B). The aforementioned data support the hypothesis that increased cell proliferation and/or maturation during the differentiation of progenitor cells into neutrophils may contribute to the neutrophilia of Wip1-deficient mice.

Myeloid progenitors originate from HSCs. According to the FcγRII/III (CD16/32) and CD34 expression levels in gated Lin<sup>-</sup>Sca1<sup>-</sup>c-Kit<sup>+</sup> cells, megakaryocyte-erythroid progenitors (MEPs, CD34<sup>low</sup>CD16/32<sup>low</sup>), common myeloid progenitors (CMPs, CD34<sup>hi</sup>CD16/32<sup>low</sup>), and GMPs (CD34<sup>hi</sup>CD16/32<sup>hi</sup>) could be distinguished.<sup>6,18,26</sup> No significant cell percentage and absolute cell number changes were disclosed in the different myeloid progenitor subpopulations isolated from the BM of Wip1KO mice compared with WT mice, although GMPs showed a tendency of increasing in Wip1-deficient mice (Figure 3A). Long-term HSCs (LT-HSCs) and multipotent progenitors (MPPs) can be detected through staining BMCs with antibodies against CD150 and CD48.<sup>27</sup> The absolute cell number and percentage of LT-HSCs and MPPs in Wip1KO mice were comparable with WT mice ( $P > .05$ , Figure 3B). These results demonstrate that there is no detectable change in the hematopoietic precursor populations in the BM of Wip1KO mice. We thus propose that Wip1 deficiency may mainly enhance the differentiation process of GMPs into neutrophils.

To directly test this possibility, we performed the methylcellulose culture analysis. Wip1-deficient BMCs generated significantly more colonies than WT BMCs in methylcellulose cultures with G-CSF ( $P < .01$ , Figure 3C). Analyses of the phenotype of the generated cells originating from Wip1-deficient purified Lin<sup>-</sup>Sca1<sup>-</sup>c-Kit<sup>+</sup>CD34<sup>hi</sup>CD16/32<sup>hi</sup> GMPs by FACS exhibited a 2-fold increase in neutrophil colonies at the expense of other myeloid cells, except that there were no significant changes in the monocyte/macrophage compartment compared with WT GMPs ( $P < .001$ , supplemental Figure 6A). Importantly, when we analyzed the developmental capacity of purified Lin<sup>-</sup>Sca1<sup>-</sup>c-Kit<sup>+</sup>CD34<sup>hi</sup>CD16/32<sup>hi</sup> GMPs when these cells were treated with G-CSF in a CFU assay, the colony number derived from Wip1-deficient GMPs was higher than WT cells ( $P < .01$ , Figure 3D). Interestingly, the colony size and cell number per colony formed

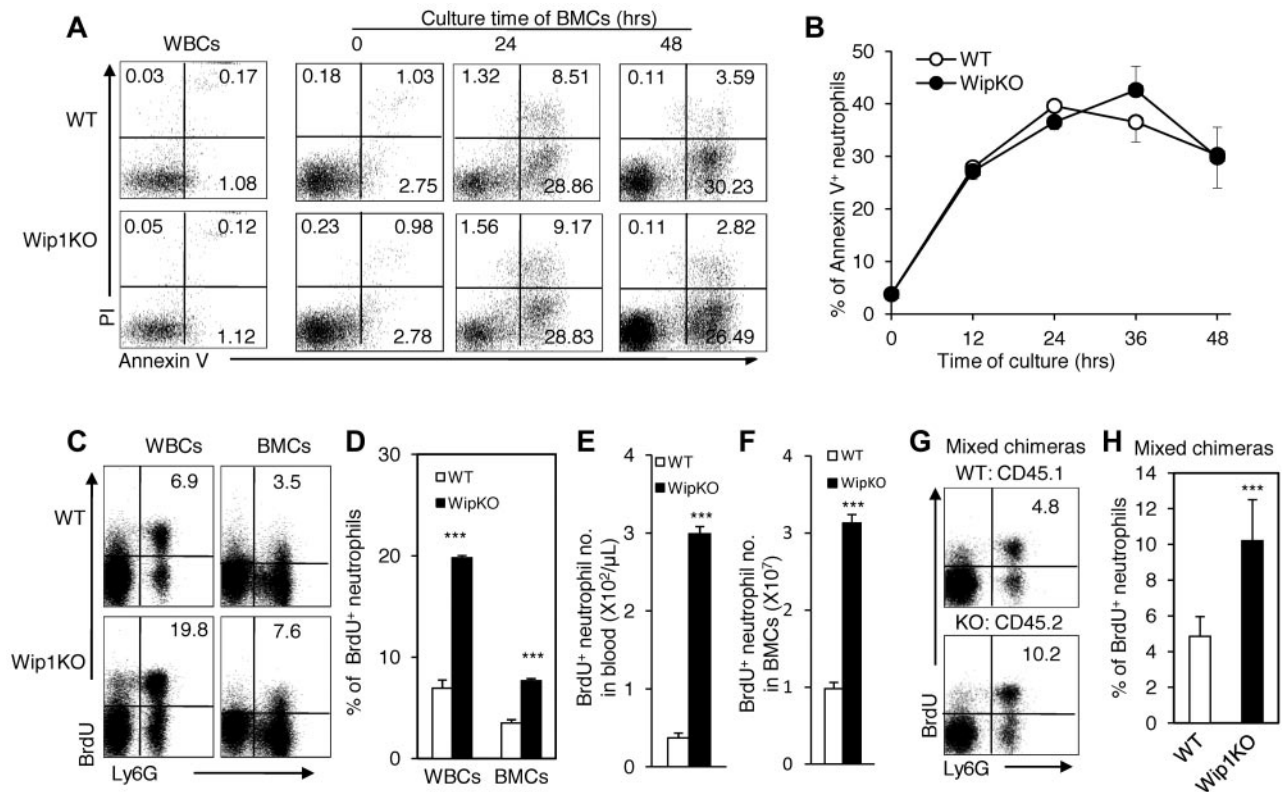


**Figure 2. Wip1-deficient neutrophils showed normal cell death but increased cell proliferation.** (A) Representative FACS analysis of blood and BM neutrophils for staining of anti-annexin-V and propidium iodide was shown. (B) Identical cell death kinetics of BM-derived neutrophils isolated from WT or Wip1KO mice was observed when cells were cultured in DMEM for different periods (mean  $\pm$  SD,  $n = 3$  for each genotype). Data are representative of 3 independent experiments. (C) BrdU incorporation in blood and BM-derived neutrophils was detected by FACS 96 hours after injection of BrdU. Increased percentage (D) and cell number (E-F) of BrdU<sup>+</sup> neutrophils in the blood and BM of Wip1KO mice were detected 96 hours after BrdU injection. Data are representative of 5 independent experiments. Generated mixed chimeric mice by transplanting either CD45.1<sup>+</sup> WT or CD45.2<sup>+</sup> Wip1KO BMCs at the ratio of 1:1 into lethally irradiated CD45.1<sup>+</sup> mice. By 6-8 weeks after BMT, BrdU were injected and BrdU<sup>+</sup> neutrophils were detected (G-H). (G) Representative FACS of BrdU<sup>+</sup> neutrophils derived from WT and Wip1KO BMCs in mixed chimeras are shown. (H) The mean neutrophil compartment percentages are analyzed 96 hours after BrdU injection (mean  $\pm$  SD,  $n = 3$  or 4). Data are representative of 3 independent experiments. \*\*\* $P < .001$  (WT vs Wip1KO).

from Wip1-deficient GMPs increased  $\sim 2$ -fold more than those from WT mice in the presence of G-CSF ( $P < .001$ , Figure 3E-F) or in the presence of GM-CSF ( $P < .001$ , supplemental Figure 6B-C). Thus, the total cell number of induced neutrophils from Wip1KO GMPs is significantly higher than those from WT controls in the presence of G-CSF ( $P < .001$ , Figure 3G).

It has been reported that the maturing neutrophils in the BM can be divided into 3 distinct populations, including CD11b<sup>int</sup>Gr-1<sup>int</sup> cells (promyelocytes/myelocytes), CD11b<sup>low</sup>Gr-1<sup>hi</sup> cells (imNeu), and CD11b<sup>hi</sup>Gr-1<sup>hi</sup> cells (mNeu) in CD11b<sup>+</sup>Gr-1<sup>+</sup> cells.<sup>23,24</sup> In accordance with the in vitro observation, we detected a significantly higher percentage of mature neutrophils and moderately lower percentages of immature neutrophils and promyelocytes/myelocytes in BMCs of Wip1-deficient mice than controls (Figure 4A-B). Moreover, Wip1-deficient neutrophils in full or mixed chimeras also revealed a higher proportion of mature phenotype and lower percentages of immature neutrophils than WT controls as determined by the expression of CD11b/Gr1 (Figure 4C-D). These results collectively indicate that Wip1 deficiency promotes neutrophil development and proliferation of granulocyte progenitors.

#### Wip1 regulates neutrophil differentiation through inhibiting the p38 MAPK-STAT1 pathway

To understand the molecular mechanisms that mediate Wip1 function in the differentiation of neutrophils, we accessed the potential pathways, including p53, p38 MAPK, signal transducer and activator of transcription-1 (STAT1), STAT3, and extracellular

receptor-activated kinase (Erk) when BMCs of control and Wip1-deficient mice were treated with GM-CSF or G-CSF by immunoblotting analysis of phosphorylated proteins. Unexpectedly, Wip1 deficiency did not cause significant p53 expression (Figure 5A). Furthermore, when we bred Wip1KO mice with p53KO mice to generate Wip1 and p53 double-knockout mice, p53 deficiency did not cause detectable changes in all stages of neutrophil maturation, whether Wip1 was expressed or not (Figure 5B). These data indicate that p53 is very unlikely to be involved in Wip1-mediated neutrophilia.

One of the early events in G-CSF or GM-CSF receptor ligation is the phosphorylation and activation of STAT3.<sup>28,29</sup> Moderately higher phosphorylation levels of STAT3 were detected in BM neutrophils of Wip1-deficient mice (Figure 5C). Notably, the phosphorylation of p38MAPK and STAT1 in Wip1-deficient cells was markedly quicker and higher than those of WT mice when these cells were stimulated with G-CSF, as determined by Western blot with neutrophils and intracellular flow cytometry assays with the sorted Lin<sup>-</sup>Sca1<sup>-</sup>c-Kit<sup>+</sup>CD34<sup>hi</sup>CD16/32<sup>hi</sup> GMPs (Figure 5C-D). Meanwhile, the phosphorylation of Erk and p-S6 in these cells was identical in Wip1KO and WT cells (Figure 5C-D). The markedly quicker and higher phosphorylation of p38MAPK and STAT1 in BM neutrophils and the sorted Wip1-deficient Lin<sup>-</sup>Sca1<sup>-</sup>c-Kit<sup>+</sup>CD34<sup>hi</sup>CD16/32<sup>hi</sup> GMPs cells was also observed when these cells were stimulated with GM-CSF (supplemental Figure 7A-B).

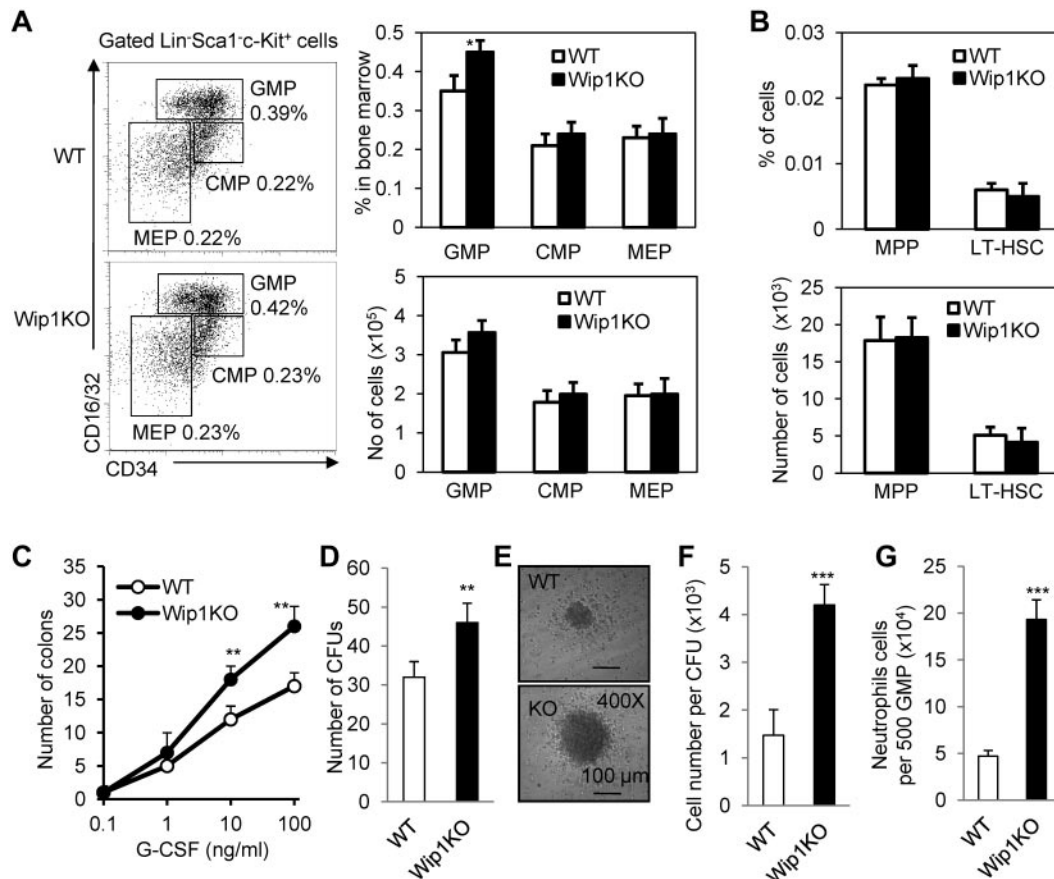


**Figure 3. Wip1 deficiency specifically promotes myeloid progenitor cell development toward the granulocyte lineage.** (A) Myeloid progenitor cell populations of 6-week-old mice were assayed by flow cytometry. Plots shown were the gated Lin<sup>-</sup>Sca1<sup>-</sup>c-kit<sup>+</sup> cells. Right panel: Percentage of whole BMCs and absolute number of progenitors per BM sample isolated from femurs and tibiae (mean  $\pm$  SD, n = 5 mice of each genotype). (B) The absolute number of MPPs and LT-HSC compartment in WT and Wip1KO mice was shown (mean  $\pm$  SD, n = 4 mice of each genotype). The expression of CD48 and CD150 were analyzed with gating Lin<sup>-</sup>Sca1<sup>+</sup>c-kit<sup>+</sup> (LSK) population. (C) Colony formation by  $4 \times 10^4$  BMCs from WT or Wip1KO mice in methylcellulose containing various concentrations of G-CSF (mean  $\pm$  SD, n = 3) was detected. Colony counts were performed at day 10. (D) A total of 500 GMPs sorted out of individual WT and Wip1KO mice were seeded in methylcellulose media supplemented with SCF and G-CSF. The experiment was performed in triplicate. Differentiated cells were analyzed by FACS at day 8 of culture. Data are the mean  $\pm$  SD. The cell numbers positive for the surface marker CD11b<sup>+</sup>F4/80<sup>-</sup>Ly6G<sup>+</sup> (neutrophils), or for CD11b<sup>+</sup>F4/80<sup>+</sup>Ly6G<sup>-</sup> (monocytes/macrophages), and CD11b<sup>-</sup>Ly6G<sup>-</sup>F4/80<sup>-</sup> (others; undifferentiated cells) were assayed. One representative CFU generated from WT or Wip1KO GMP after culture with G-CSF was photographed and is presented (E). Scale bars represent 100  $\mu$ m. (F) The neutrophil cell number per CFU was calculated. (G) The neutrophil cell number per 500 GMPs was calculated. Data are representative of 3 independent experiments. Data presented are mean  $\pm$  SD. \* $P$  < .05, compared with WT controls. \*\* $P$  < .01, compared with WT controls. \*\*\* $P$  < .001, compared with WT controls.

We detected the mRNA and protein levels of CCAAT/enhancer binding protein- $\alpha$  (C/EBP $\alpha$ ), PU.1 and GATA-1, which are the essential transcription factors in regulating the granulocytogenesis cell fate decision.<sup>30</sup> It is probable that the subsequent decision between granulocyte and monocyte commitment is determined by the balance between C/EBP $\alpha$  and PU.1.<sup>31</sup> The C/EBP $\alpha$  expression is clearly higher and PU.1 and GATA-1 expression is comparable in BM neutrophils of Wip1KO mice compared with WT mice (Figure 5E). The sorted Lin<sup>-</sup>Sca1<sup>-</sup>c-kit<sup>+</sup> CD34<sup>hi</sup>CD16/32<sup>hi</sup> GMPs of Wip1KO mice showed significantly higher C/EBP $\alpha$  expression than WT cells as determined by intracellular flow cytometry assays (Figure 5F). Importantly, sorted Wip1-deficient neutrophils from mixed chimeras also showed significantly enhanced C/EBP $\alpha$  expression (data not shown), indicating that the up-regulated C/EBP $\alpha$  expression in Wip1-deficient neutrophils is an intrinsic event. Moreover, C/EBP $\beta$  and C/EBP $\epsilon$ ,<sup>6,32</sup> which are important in regulating neutrophil maturation, particularly in the expression of granule proteins, were also clearly up-regulated in neutrophils of Wip1KO mice (Figure 5E). Consistently, the expression of G-CSF receptor, which is reported to be regulated by C/EBP $\alpha$ ,<sup>33</sup> was also significantly higher in Wip1-deficient neutrophils (supplemental Figure 8).

STAT3 is involved in the differentiation of neutrophils.<sup>28,29</sup> To determine whether the moderately enhanced p-STAT3 in Wip1KO neutrophils mediates the accelerated differentiation of neutrophils from Wip1KO GMPs, we studied the neutrophil development when WT and Wip1KO GMPs were cultured with G-CSF in the presence of STAT3 inhibitor S3I-201 (NSC 74859, Santa Cruz Biotechnology) in CFU assays. Inhibiting STAT3 did decrease neutrophil differentiation from WT GMPs (supplemental Figure 9). However, inhibiting STAT3 failed to rescue the enhanced neutrophil differentiation from Wip1KO mice (supplemental Figure 9). These data indicate that STAT3 is unlikely to be involved in the enhanced differentiation of neutrophils in Wip1KO mice. Is the p38 MAPK-STAT1 pathway involved in Wip1-mediated regulation on neutrophil differentiation? To address this issue, we observed the neutrophil development from WT and Wip1KO GMPs when these GMPs were cultured with G-CSF in the presence of p38 MAPK and Jnk activator (10  $\mu$ M anisomycin) and/or Jnk inhibitor (100nM SP600125). Selective activation of p38 MAPK by anisomycin and SP600125 significantly increased the C/EBP $\alpha$  expression in WT GMPs in the presence of G-CSF ( $P$  < .001, Figure 6A). Simultaneously, p38 MAPK activation increased the number and size of CFUs as well as the total neutrophil cell numbers from WT GMPs ( $P$  < .001,

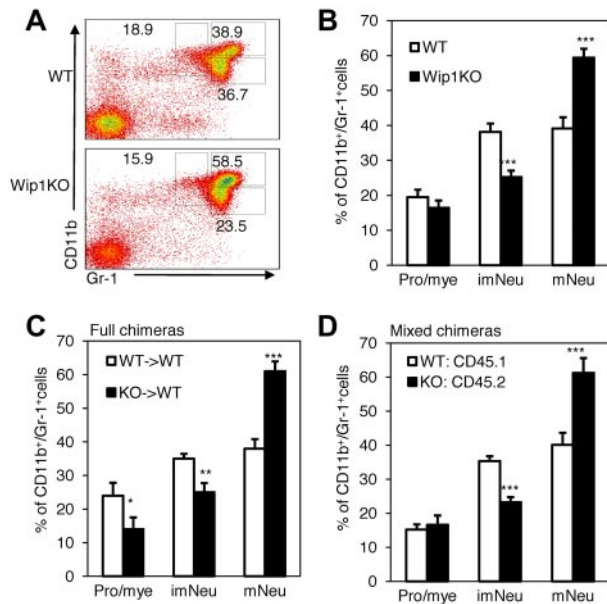


**Figure 4. Accelerated maturation of BM-derived neutrophils in Wip1-deficient mice.** (A) The maturation of granulocytes in BMCs can be distinguished by the expression of CD11b/Gr-1. Three populations can be achieved: CD11b<sup>int</sup>Gr-1<sup>int</sup> cells (promyelocyte/myelocyte neutrophils), CD11b<sup>hi</sup>Gr-1<sup>hi</sup> cells (mature neutrophils), and CD11b<sup>low</sup>Gr-1<sup>hi</sup> cells (immature neutrophils). One representative FACS analysis of BM CD11b<sup>+</sup>Gr-1<sup>+</sup> neutrophils was shown. (B) The neutrophil maturation phenotype of WT or Wip1KO mice was analyzed on freshly isolated and erythrocyte-depleted BMCs. Represented is one of 5 independent experiments with similar results. The percentage of cells in the different developing stages among CD11b<sup>+</sup>Gr-1<sup>+</sup> cells in full (C) or mixed chimeric (D) mice were analyzed by FACS. Chimeras were generated by transplanting either CD45.2<sup>+</sup> WT or Wip1KO BM into CD45.1<sup>+</sup> lethally irradiated mice as described in "Methods." Data are mean  $\pm$  SD and are representative from 3 independent experiments. \* $P < .05$ , compared with WT controls. \*\* $P < .01$ , compared with WT controls. \*\*\* $P < .001$ , compared with WT controls.

Figure 6B-E). Furthermore, we observed the neutrophil development from either WT or Wip1KO GMPs when these GMPs were treated with G-CSF in the presence of SB203580 (10 $\mu$ M, p38 inhibitor), MTA (5 $\mu$ M, STAT1 inhibitor), and U0126 (10 $\mu$ M Erk inhibitor). The agents efficiently inhibited p38 MAPK, STAT1, and Erk activity in BM neutrophils induced by G-CSF as determined by Western blot assays (supplemental Figure 10). As shown in Figure 6, inhibition of p38 MAPK and/or STAT1 significantly reversed the up-regulated C/EBP $\alpha$  expression in Wip1-deficient neutrophils (Figure 6F) and rescued the enhanced differentiation and developments of neutrophils from Wip1KO GMPs as determined by colony formation and neutrophil number (Figure 6G-J). In contrast, treatment with U0126 failed to do so (Figure 6G-J). Similar studies using p38 MAPK and STAT1 inhibitors showed that the involvement of p38 MAPK-STAT1 in neutrophil development induced by GM-CSF in vitro (supplemental Figure 11). To further determine the role of p38 MAPK-STAT1 in the development of neutrophils, we observed the neutrophil development of GMPs isolated from p38<sup>+/-</sup> mice or GMPs with a knockdown STAT1 expression by RNAi technique. G-CSF induced less p38 and STAT1 activity in P38<sup>+/-</sup> GMPs compared with WT controls (Figure 7A). Consistent with the results observed with p38 MAPK inhibitor, decreased p38 MAPK activity caused a significantly decreased neutrophil development efficiency, as indicated by the smaller colony size, reduced cell number per colony, and a lesser total neutrophil number (Figure 7B-E). Knockdown STAT1 using shRNA decreased STAT1 expression (Figure 7F) and significantly rescued the enhanced neutrophil development caused by Wip1 deficiency (Figure 7G-J). Therefore,

higher activities of p38 MAPK-STAT1-C/EBP $\alpha$  pathways in Wip1KO mice probably potentiate the differentiation of neutrophils.

## Discussion

In the present study, we provide evidence that expression of Wip1 is dynamically regulated in neutrophils across the whole development spectrum with the highest expression in resting mature neutrophils, thus demonstrating a key role for this phosphatase in the control of neutrophil development and function (supplemental Figure 12). Specifically, Wip1 delivers a myeloid-specific intrinsic signal in repressing BM neutrophil differentiation as evidenced by our systemic analysis of Wip1-deficient mice, mixed chimeras, and colon formation experiments of the sorted GMP cells. In our results, GMPs isolated from Wip1-deficient mice preferentially developed into granulocytes at the expense of monocytes/macrophages and undifferentiated cells when cultivated in the presence of GM-CSF or G-CSF. Consistent with the in vitro results, no significant percentage and absolute cell number changes were disclosed in LT-HSCs, MPPs as well as myeloid progenitor subpopulations, including MEPs, CMPs, and GMPs in the BM of Wip1KO mice were comparable with control mice. However, a significantly higher percentage of mature neutrophils (CD11b<sup>hi</sup>Ly6G<sup>hi</sup>) and moderately lower percentages of immature neutrophils (CD11b<sup>low</sup>Ly6G<sup>hi</sup>) and promyelocytes/myelocytes (CD11b<sup>int</sup>Ly6G<sup>int</sup>) were observed in the BM of Wip1-deficient mice than controls. The accelerated differentiation to neutrophils was also supported by the enhanced BrdU incorporation into mature neutrophils in vivo. In addition to the increased cell number of neutrophils in Wip1-deficient mice, neutrophils in these mice displayed significant hypermature phenotypes. Putting all these data together, we arrived at the conclusion that Wip1 negatively modulates the neutrophil differentiation process and maturation state from its progenitor cells in an intrinsic manner.

The peripheral neutrophil pool is nicely maintained in steady state with an extensive production and quick cell death in mice and humans.<sup>34</sup> Wip1-deficient mice showed severe neutrophilia. The enhanced neutrophil lineage differentiation in Wip1-deficient mice is probably the key reason for the neutrophilia in these mice, as supported by the following evidence: (1) neutrophil development was largely accelerated in the BM of Wip1 deficient mice; (2) immature and mature neutrophils in the BM of Wip1-deficient mice expressed higher CXCR2 and lower CXCR4 than those in control mice (data not shown). The balance of CXCR2 and CXCR4 controls the release of neutrophils from BM.<sup>35</sup> The increased ratio of CXCR2 and CXCR4 in Wip1-deficient mice probably caused a shift in the pool of mature neutrophils from BM to circulation; and (3) neutrophils from Wip1KO mice showed identical cell death ratio as control mice as determined by annexin V and propidium iodide staining. In addition, cell death-related gene p53-deficient mice showed normal neutrophil pool as control mice, excluding the possibility that Wip1-mediated p53 pathway may affect the life span of circulating neutrophils.

To identify the molecular mechanisms that mediate the "breaker" function of Wip1 in neutrophil differentiation, we examined signaling pathways potentially activated by Wip1 in neutrophils. We found that Wip1 deficiency mainly caused the enhanced activation of p38 MAPK-STAT1, but not Erk, p53, and Jnk in BM and circulating neutrophils after G-CSF or GM-CSF stimulation. Notably, using specific pharmacologic inhibitors or genetic modification methods, inhibiting p38 MAPK or STAT1 remarkably rescued Wip1 deficiency-induced differentiation of neutrophils,

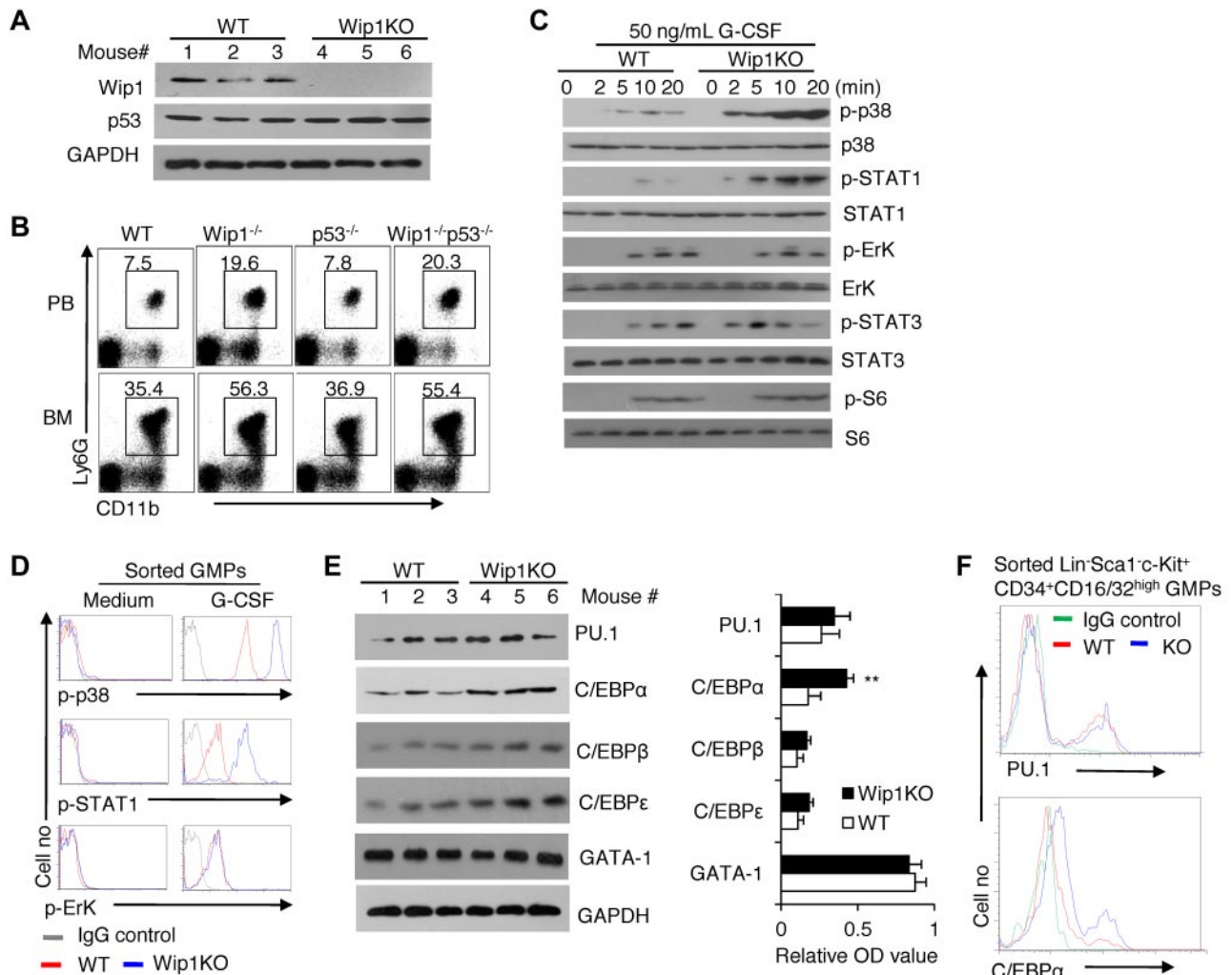


**Figure 5. Wip1 deficiency promotes the development of neutrophils in a p53-independent manner but increases the expression of granulopoiesis-related transcription factors and p38 MAPK-STAT1.** (A) BMCs of WT and Wip1KO mice were lysed and analyzed for the expression of Wip1 and p53 by immunoblotting. Data are representative of 3 independent experiments. (B) Representative FACS analysis of peripheral blood and BM CD11b<sup>+</sup>Ly6G<sup>+</sup> neutrophils from WT, Wip1<sup>-/-</sup>, p53<sup>-/-</sup>, and p53<sup>-/-</sup>Wip1<sup>-/-</sup> were shown; represented is 1 of 3 independent experiments with similar results. (C) Erythrocyte-depleted BMCs of WT and Wip1KO mice were treated with G-CSF for the indicated time. Cells were lysed and analyzed by immunoblotting for the phosphorylation of p38 MAPK (p-p38), Erk (p-Erk), STAT1 (p-STAT1), STAT3 (p-STAT3), and S6 (p-S6), as well as for the total amount of proteins used for analysis. (D) Activation of p38 MAPK, STAT1, and Erk in sorted WT and Wip1KO GMPs stimulated with medium alone or G-CSF, assessed by FACS with phosphorylation-specific antibodies. (E) BM neutrophils of WT and Wip1KO mice were lysed and analyzed for the transcription factor expression of PU.1, GATA-1, and C/EBPα, β, and ε by immunoblotting. Three mice in each group were assayed. The averages of the relative OD value were summarized (right panel). \*\**P* < .01, compared with WT mice. (F) The expression of PU.1 and C/EBPα in GMPs of WT and Wip1KO mice was analyzed by FACS.

indicating that Wip1 regulated neutrophil differentiation via p38 MAPK-STAT1 pathway. It is worth noting that p38 MAPK may regulate other downstream target molecules in addition to STAT1 to regulate neutrophil development; on the other hand, STAT1 may be regulated by additional upstream molecules, except for p38 MAPK during neutrophil differentiation. This issue should be addressed in the coming studies. However, it is somewhat inconsistent with the recent report showing that p38 MAPK plays a differential role in regulating neutrophil and eosinophil progenitor expansion and inhibits neutrophil development in isolated human CD34<sup>+</sup> cells.<sup>36</sup> The reasons for the discrepancy are not clear. It is probable that p38 MAPK may play distinct roles in different stages of granulocytic differentiation. It is reported that phosphorylation of p38 MAPK is involved in a defect in the maintenance of HSC quiescence caused by the elevated reactive oxygen species level.<sup>37</sup> However, our results showed that the expression of Wip1 in HSCs is low but increased dynamically during neutrophil development. Wip1-deficient mice did not show detectable alteration of LT-HSCs, MPPs, MEPs, CMPs, and GMPs. Therefore, Wip1 defi-

ciency may mainly alter the p38 MAPK activity in committed granulocytic progenitor cells or promyelocytes/myelocytes (CD11b<sup>int</sup>Ly6G<sup>int</sup>) but not those in the stem cell pool. On the other hand, it is reported that myeloid cell fate choice is determined by the relative concentration of transcription factors, especially the balance between C/EBPα and PU.1.<sup>31</sup> Our present data showed that Wip1-deficient GMPs expressed more C/EBPα, C/EBPβ, and C/EBPε but similar levels of PU.1 and GATA1 compared with WT mice. The enhanced ratio of C/EBPα to PU.1 as well as the increased G-CSF receptor expression, one of the important target molecules for C/EBPα and PU.1,<sup>33</sup> may explain the neutrophilia phenotype of Wip1-deficient mice. Furthermore, molecular and biochemical analysis indicated that Wip1 down-regulated the P38 MAPK-STAT1 pathway to inhibit C/EBPα and finally to block granulocytogenesis, although other signaling pathways could not be excluded at this moment. Nevertheless, we identified Wip1 as a neutrophil lineage-specific regulator mainly via p38 MAPK-STAT1-C/EBPα pathway.

It is demonstrated that the activity of p53, which plays a central role in preserving genomic integrity, is one of the key target

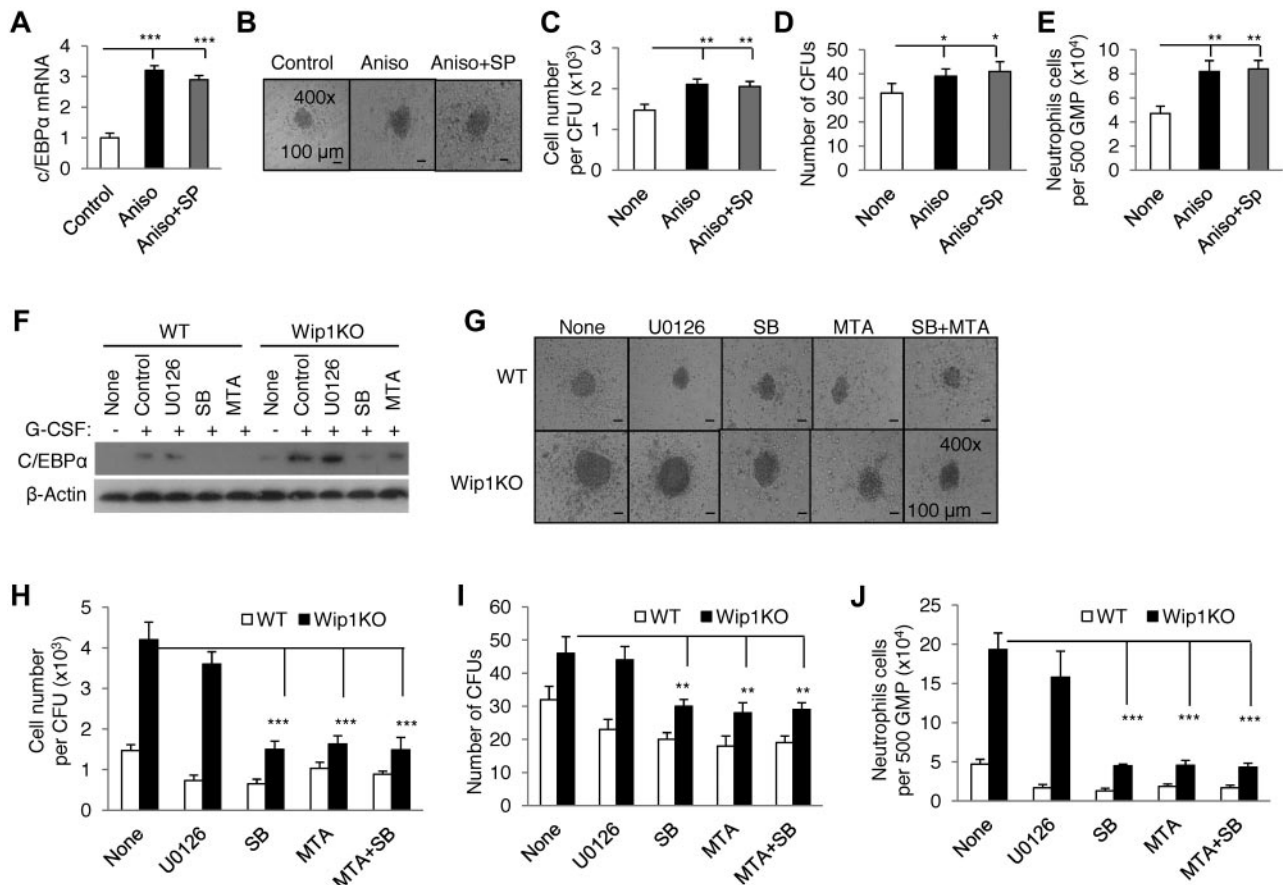


**Figure 6. Inhibiting p38 MAPK-STAT1 significantly rescued Wip1 deficiency-caused accelerated neutrophil development.** (A) Sorted WT GMPs were treated with G-CSF in the presence or absence of 10  $\mu$ M anisomycin (activator of p38 and Jnk) and/or 100 nM SP600125 (inhibitor of Jnk). The transcriptional factor C/EBP $\alpha$  mRNA expression was detected by real-time PCR. One photographed CFU (B), neutrophil number per CFU (C), number of CFUs (D), and neutrophil number of per 500 GMPs (E) were shown. (F) Erythrocyte-depleted BMCs of WT and Wip1KO mice were treated with G-CSF in the presence or absence of 10  $\mu$ M U0126 (inhibitor of Erk), 5  $\mu$ M SB203580 (inhibitor of p38), 10  $\mu$ M MTA (inhibitor of STAT1), and the transcriptional factor C/EBP $\alpha$  expression were detected by immunoblotting. (G) A total of 500 GMPs sorted from WT and Wip1KO mice were seeded in methylcellulose media supplemented with SCF, IL-3, and G-CSF in the presence or absence of U0126, SB203580, or MTA. The experiment was performed in triplicate. One CFU with a representative size generated from WT or Wip1KO GMPs was photographed. Absolute neutrophil number per CFU (H), number of CFUs (I), and neutrophil number of per 500 GMPs (J) were detected after 8 days in culture. Data (mean  $\pm$  SD) are one of 2 independent experiments with similar results. \* $P$  < .05, between the indicated groups. \*\* $P$  < .01, between the indicated groups. \*\*\* $P$  < .001 between the indicated groups.

molecules attenuated by Wip1 in many different type cells.<sup>38,39</sup> However, we failed to detect the alteration of p53 activity in neutrophils of Wip1-deficient mice. Importantly, p53<sup>-/-</sup> mice showed similar levels and function of neutrophils as WT mice. Wip1<sup>-/-</sup>p53<sup>-/-</sup> mice displayed identical levels and function of neutrophils in BM and peripheral blood as Wip1<sup>-/-</sup> mice. Therefore, Wip1 negatively controls neutrophils via a p53-independent approach. It is sharply distinct from the positive regulating role of Wip1 in T-cell development in the thymus, which is dependent on the presence of p53<sup>40</sup> and its oncogene activity.<sup>8</sup> The opposite effects of Wip1 on neutrophils and other cells, such as T cells, tumor cells, and others, may be the result of the distinct expression pattern of Wip1 and the different roles of p53 and p38 MAPK pathways in these cells.

It is interesting to note that microRNA-223 and carcinoembryonic antigen-related cell adhesion molecule-1 critically regulate GMPs or even earlier progenitors.<sup>26,41</sup> However, Wip1 may mainly regulate the relatively late stage of neutrophil development from its progenitor cells. It is somewhat consistent with the observation that Wip1 expression increases during the differentiation of GMPs into mature neutrophils, whereas HSCs express low levels of Wip1. The detailed studies on the possible involvement of Wip1 in the

maintenance and differentiation progression of progenitor cells are still recommended.

In conclusion, the expression of phosphatase Wip1 was regulated dynamically during neutrophil development. Our data support a model in which Wip1 acts as a key negative fine-tuner of the development, maturation, and homeostasis of granulocytic cells mainly by the p38 MAPK-STAT1-C/EBP $\alpha$  pathway. Wip1, as the phosphatase identified to be an intrinsic-negative master for neutrophils, may be a promising target for therapeutic intervention to modulate neutrophil function in its related diseases.

## Acknowledgments

The authors thank Drs Xian C. Li, Nickolas Nahm, Hanhan Li, and Douglas Corley for kind review of the manuscript; Mrs Jing Wang, Mr Yabing Liu, and Mrs Xiaoqiu Liu for expert technical assistance; Mrs Qinghuan Li and Jianxia Peng for excellent laboratory management; and Mr Baisheng Ren for outstanding animal husbandry.

This work was supported by the National Basic Research Program of China (grants 2010CB945301 and 2011CB710900, Y.Z.), the National Natural Science Foundation (grants C81130055, C81072396, and U0832003; Y.Z.; grants C31171407 and

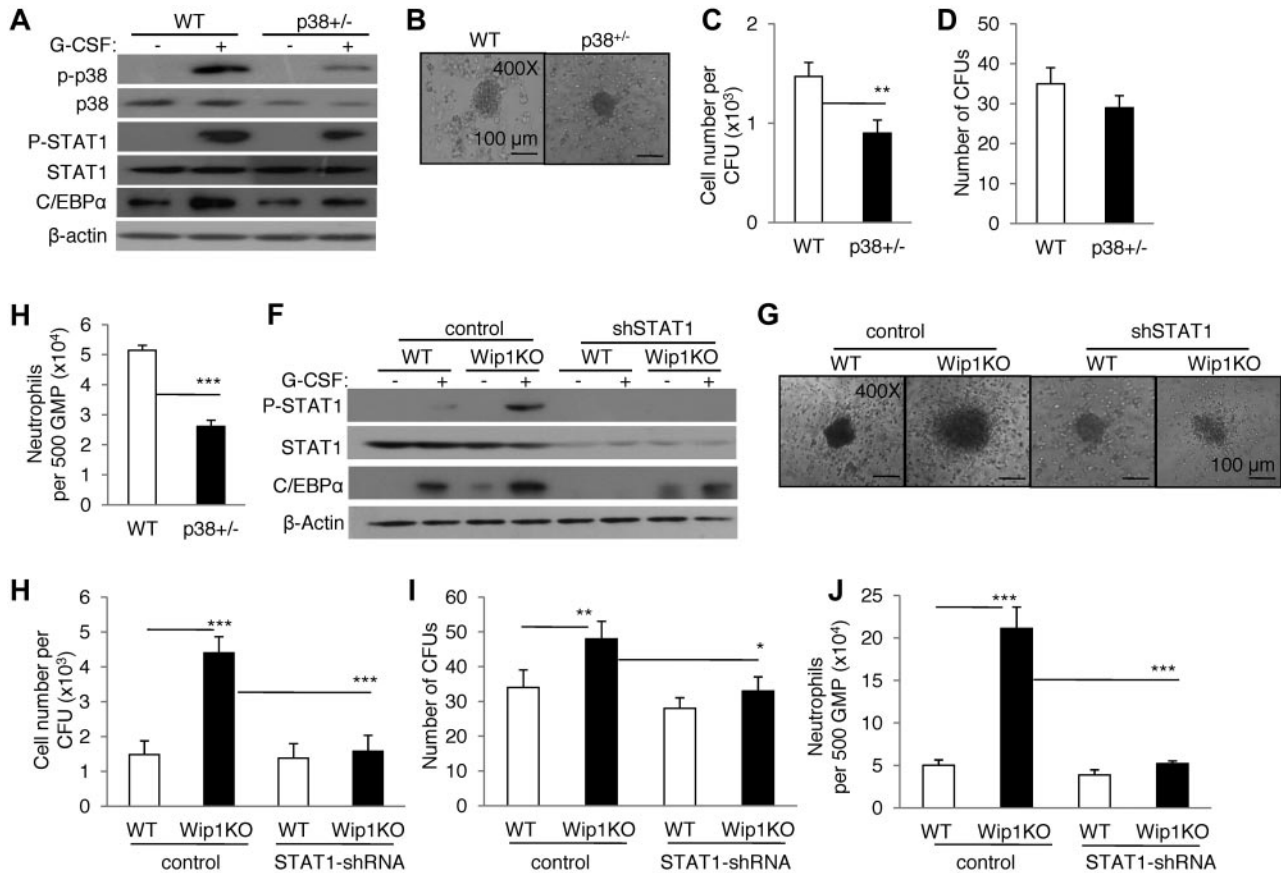


**Figure 7. Knockdown p38 MAPK-STAT1 by genetic modification significantly reversed the enhanced neutrophil development caused by Wip1 deficiency.** (A) Erythrocyte-depleted BMCs of WT and p38<sup>+/-</sup> mice were treated with G-CSF, and the expression of p38 MAPK, STAT1, and C/EBP $\alpha$  was detected by immunoblotting. (B) A total of 500 GMPs sorted from WT and Wip1KO mice were seeded in methylcellulose media supplemented with SCF, IL-3, and G-CSF. The experiment was performed in triplicate. One representative CFU generated from WT or p38<sup>+/-</sup> GMPs was photographed. Absolute neutrophil number per CFU (C), number of CFUs (D), and neutrophil number of per 500 GMPs (E) were detected after 8 days in culture. Data (mean  $\pm$  SD) are one of 2 independent experiments with similar results. \* $P$  < .05, between the indicated groups. \*\* $P$  < .01, between the indicated groups. \*\*\* $P$  < .001, between the indicated groups. (F) Sorted GMPs of WT and Wip1KO mice were transfected with control and STAT1 shRNA vectors and further treated with G-CSF. The expression of STAT1 and C/EBP $\alpha$  was detected by Western blotting. (G-J) A total of 500 sorted WT and Wip1-deficient GMPs expressing either control or STAT1 shRNA vector were seeded in methylcellulose media supplemented with SCF, IL-3, and G-CSF; the colony-forming assays were then performed. One representative CFU generated in each group was photographed (G). Absolute neutrophil number per CFU (H), number of CFUs (I), and neutrophil number of per 500 GMPs (J) were detected after 8 days in culture. Data (mean  $\pm$  SD) are one of 2 independent experiments with similar results. \* $P$  < .05, between the indicated groups. \*\* $P$  < .01, between the indicated groups. \*\*\* $P$  < .001, between the indicated groups.

C81273201, G.L.), and the Chinese Academy of Sciences for Distinguished Young Scientists (KSCX2-EW-Q-7; G.L. and Key Basic Research Project of the Science and Technology Commission of Shanghai Municipality (12JC1400900; G.L.).

## Authorship

Contribution: G.L. designed and performed the experiments with cells and mice, analyzed data, and contributed to writing the manuscript; X.H. designed and performed the experiments with cells and mice, analyzed data, and contributed to managing the mouse colonies; B.S. performed the cell signal assays with immunoblotting methods; T.Y. performed some Western blot assays; J.S. analyzed histologic data; L.Z. provided animal models and

revised the manuscript; and Y.Z. designed experiments, analyzed data, wrote the manuscript, and provided overall direction.

Conflict-of-interest disclosure: The authors declare no competing financial interests.

Correspondence: Yong Zhao, Transplantation Biology Research Division, State Key Laboratory of Biomembrane and Membrane Biotechnology, Institute of Zoology, Chinese Academy of Sciences, Beichen Xi Road 1-5, Chaoyang District, Beijing, China 100101; e-mail: zhaoy@ioz.ac.cn; and Lianfeng Zhang, Key Laboratory of Human Diseases Comparative Medicine, Ministry of Health, Institute of Laboratory Animal Science, Chinese Academy of Medical Sciences and Peking Union Medical College, Chaoyang District, Pan Jia Yuan Nan Li No. 5, Beijing, China 100021; e-mail: zhanglf@cnilas.org.

## References

1. Metcalf D. Stem cells, pre-progenitor cells and lineage-committed cells: are our dogmas correct? *Ann N Y Acad Sci*. 1999;872:289-303.
2. Amulic B, Cazalet C, Hayes GL, Metzler KD, Zychlinsky A. Neutrophil function: from mechanisms to disease. *Annu Rev Immunol*. 2012;30:459-489.
3. Mantovani A, Cassatella MA, Costantini C, Jaillon S. Neutrophils in the activation and regulation of innate and adaptive immunity. *Nat Rev Immunol*. 2011;11(8):519-531.
4. Brinkmann V, Reichard U, Goosmann C, et al. Neutrophil extracellular traps kill bacteria. *Science*. 2004;303(5663):1532-1535.
5. Demetri GD, Griffin JD. Granulocyte colony-stimulating factor and its receptor. *Blood*. 1991; 78(11):2791-2808.
6. Borregaard N. Neutrophils, from marrow to microbes. *Immunity*. 2010;33(5):657-670.
7. Fiscella M, Zhang H, Fan S, et al. Wip1, a novel human protein phosphatase that is induced in response to ionizing radiation in a p53-dependent

- manner. *Proc Natl Acad Sci U S A*. 1997;94(12):6048-6053.
8. Le Guezennec X, Bulavin DV. WIP1 phosphatase at the crossroads of cancer and aging. *Trends Biochem Sci*. 2010;35(2):109-114.
  9. Salminen A, Kaarimäntä K. Control of p53 and NF- $\kappa$ B signaling by WIP1 and MIF: role in cellular senescence and organismal aging. *Cell Signal*. 2011;23(5):747-752.
  10. Chew J, Biswas S, Shreeram S, et al. WIP1 phosphatase is a negative regulator of NF- $\kappa$ B signalling. *Nat Cell Biol*. 2009;11(5):659-666.
  11. Lu X, Nguyen TA, Moon SH, Darlington Y, Sommer M, Donehower LA. The type 2C phosphatase Wip1: an oncogenic regulator of tumor suppressor and DNA damage response pathways. *Cancer Metastasis Rev*. 2008;27(2):123-135.
  12. Oliva-Trastoy M, Berthonaud V, Chevalier A, et al. The Wip1 phosphatase (PPM1D) antagonizes activation of the Chk2 tumour suppressor kinase. *Oncogene*. 2007;26(10):1449-1458.
  13. Bulavin DV, Phillips C, Nannenga B, et al. Inactivation of the Wip1 phosphatase inhibits mammary tumorigenesis through p38 MAPK-mediated activation of the p16(Ink4a)-p19(Arf) pathway. *Nat Genet*. 2004;36(4):343-350.
  14. Choi J, Nannenga B, Demidov ON, et al. Mice deficient for the wild-type p53-induced phosphatase gene (Wip1) exhibit defects in reproductive organs, immune function, and cell cycle control. *Mol Cell Biol*. 2002;22(4):1094-1105.
  15. Liu G, Burns S, Huang G, et al. The receptor S1P1 overrides regulatory T cell-mediated immune suppression through Akt-mTOR. *Nat Immunol*. 2009;10(7):769-777.
  16. Liu G, Duan K, Ma H, Niu Z, Peng J, Zhao Y. An instructive role of donor macrophages in mixed chimeras in the induction of recipient CD4(+)Foxp3(+) Treg cells. *Immunol Cell Biol*. 2011;89(8):827-835.
  17. Kondo M, Weissman IL, Akashi K. Identification of clonogenic common lymphoid progenitors in mouse bone marrow. *Cell*. 1997;91(5):661-672.
  18. Akashi K, Traver D, Miyamoto T, Weissman IL. A clonogenic common myeloid progenitor that gives rise to all myeloid lineages. *Nature*. 2000;404(6774):193-197.
  19. Miller CL, Lai B. Human and mouse hematopoietic colony-forming cell assays. *Methods Mol Biol*. 2005;290:71-89.
  20. Liu G, Yang K, Burns S, Shrestha S, Chi H. The S1P(1)-mTOR axis directs the reciprocal differentiation of T(H)1 and T(reg) cells. *Nat Immunol*. 2010;11(11):1047-1056.
  21. Rothe G, Emmendorffer A, Oser A, Roesler J, Valet G. Flow cytometric measurement of the respiratory burst activity of phagocytes using dihydrorhodamine 123. *J Immunol Methods*. 1991;138(1):133-135.
  22. Buser C, Walther P. Freeze-substitution: the addition of water to polar solvents enhances the retention of structure and acts at temperatures around -60 degrees C. *J Microsc*. 2008;230(2):268-277.
  23. Ueda Y, Kondo M, Kelsoe G. Inflammation and the reciprocal production of granulocytes and lymphocytes in bone marrow. *J Exp Med*. 2005;201(11):1771-1780.
  24. Fiedler K, Sindrilaru A, Terszowski G, et al. Neutrophil development and function critically depend on Bruton tyrosine kinase in a mouse model of X-linked agammaglobulinemia. *Blood*. 2011;117(4):1329-1339.
  25. Basu S, Hodgson G, Katz M, Dunn AR. Evaluation of role of G-CSF in the production, survival, and release of neutrophils from bone marrow into circulation. *Blood*. 2002;100(3):854-861.
  26. Johnnidis JB, Harris MH, Wheeler RT, et al. Regulation of progenitor cell proliferation and granulocyte function by microRNA-223. *Nature*. 2008;451(7182):1125-1129.
  27. Kim I, He S, Yilmaz OH, Kiel MJ, Morrison SJ. Enhanced purification of fetal liver hematopoietic stem cells using SLAM family receptors. *Blood*. 2006;108(2):737-744.
  28. Nguyen-Jackson H, Panopoulos AD, Zhang H, Li HS, Watowich SS. STAT3 controls the neutrophil migratory response to CXCR2 ligands by direct activation of G-CSF-induced CXCR2 expression and via modulation of CXCR2 signal transduction. *Blood*. 2010;115(16):3354-3363.
  29. Zhang H, Nguyen-Jackson H, Panopoulos AD, Li HS, Murray PJ, Watowich SS. STAT3 controls myeloid progenitor growth during emergency granulopoiesis. *Blood*. 2010;116(14):2462-2471.
  30. Radomska HS, Huettner CS, Zhang P, Cheng T, Scadden DT, Tenen DG. CCAAT/enhancer binding protein alpha is a regulatory switch sufficient for induction of granulocytic development from bipotential myeloid progenitors. *Mol Cell Biol*. 1998;18(7):4301-4314.
  31. Dahl R, Walsh JC, Lancki D, et al. Regulation of macrophage and neutrophil cell fates by the PU.1:C/EBPalpha ratio and granulocyte colony-stimulating factor. *Nat Immunol*. 2003;4(10):1029-1036.
  32. Yamanaka R, Barlow C, Lekstrom-Himes J, et al. Impaired granulopoiesis, myelodysplasia, and early lethality in CCAAT/enhancer binding protein epsilon-deficient mice. *Proc Natl Acad Sci U S A*. 1997;94(24):13187-13192.
  33. Smith LT, Hohaus S, Gonzalez DA, Dziennis SE, Tenen DG. PU.1 (Spi-1) and C/EBP alpha regulate the granulocyte colony-stimulating factor receptor promoter in myeloid cells. *Blood*. 1996;88(4):1234-1247.
  34. Summers C, Rankin SM, Condliffe AM, Singh N, Peters AM, Chilvers ER. Neutrophil kinetics in health and disease. *Trends Immunol*. 2010;31(8):318-324.
  35. Eash KJ, Greenbaum AM, Gopalan PK, Link DC. CXCR2 and CXCR4 antagonistically regulate neutrophil trafficking from murine bone marrow. *J Clin Invest*. 2010;120(7):2423-2431.
  36. Geest CR, Buitenhuis M, Laarhoven AG, et al. p38 MAP kinase inhibits neutrophil development through phosphorylation of C/EBPalpha on serine 21. *Stem Cells*. 2009;27(9):2271-2282.
  37. Ito K, Hirao A, Arai F, et al. Reactive oxygen species act through p38 MAPK to limit the lifespan of hematopoietic stem cells. *Nat Med*. 2006;12(4):446-451.
  38. Takekawa M, Adachi M, Nakahata A, et al. p53-inducible wip1 phosphatase mediates a negative feedback regulation of p38 MAPK-p53 signaling in response to UV radiation. *EMBO J*. 2000;19(23):6517-6526.
  39. Lu X, Ma O, Nguyen TA, Jones SN, Oren M, Donehower LA. The Wip1 phosphatase acts as a gatekeeper in the p53-Mdm2 autoregulatory loop. *Cancer Cell*. 2007;12(4):342-354.
  40. Schito ML, Demidov ON, Saito S, Ashwell JD, Appella E. Wip1 phosphatase-deficient mice exhibit defective T cell maturation due to sustained p53 activation. *J Immunol*. 2006;176(8):4818-4825.
  41. Pan H, Shively JE. Carcinoembryonic antigen-related cell adhesion molecule-1 regulates granulopoiesis by inhibition of granulocyte colony-stimulating factor receptor. *Immunity*. 2010;33(4):620-631.